Supplementary Information (SI) for Journal of Materials Chemistry A.

Supporting Information

Enhancing Carbon Dioxide Capture under Humid Conditions by Optimizing Pore Surface Structure

Guoyu Zhang [a], Feng Xie [a], Saif Ullah [b], Lulu Ma [c], Simon J. Teat [d], Shengqian Ma [e], Timo Thonhauser [b], Kui Tan [e], Hao Wang [c]*, and Jing Li [a]*

[a] Department of Chemistry and Chemical Biology, Rutgers University, 123 Bevier Road, Piscataway, New Jersey 08854, United States
[b] Department of Physics and Center for Functional Materials, Wake Forest University, 1834 Wake Forest Road, Winston–Salem, North Carolina 27109, United States
[c] Hoffmann Institute of Advanced Materials, Shenzhen Polytechnic, 7098 Liuxian Boulevard, Shenzhen, Guangdong 518055, PR China
[d] Advanced Light Source Lawrence Berkeley National Laboratory, 1 Cyclotron Road, Berkeley, California 94720, United States
[e] Department of Chemistry, University of North Texas, 1155 Union Cir, Denton, Texas 76203, United States

Table of Contents

S1. Materials

Reagents and solvents were used as received from: *Alfa-Aesar*: Zinc nitrate hexahydrate (98%), Nickel nitrate hexahydrate (97%), Cobalt nitrate tetrahydrate (97%), Copper nitrate dihydrate (98%), 9,10-Dibromoanthracene (99%+), Dichloromethane (99.5%), Methanol (99.9%), DMF (99%) Ethyl acetate (99%), Ether (99%); *Acros Organics*: n-Butyllithium (1.6 M in hexane), Sodium hydroxide (99%); *Ambeed*: Potassium permanganate (99%), 1,4-Diazabicyclo[2,2,2]octane (97%), 1,4-Benzenedicarboxylic acid (98%), 1,4-Naphthalenedicarboxylic acid (98%); *VWR*: Hydrochloric acid (36.5%-38%); PraxAir: N_2 (99.99%), CO_2 (99.9%)

S2. Ligand Characterization

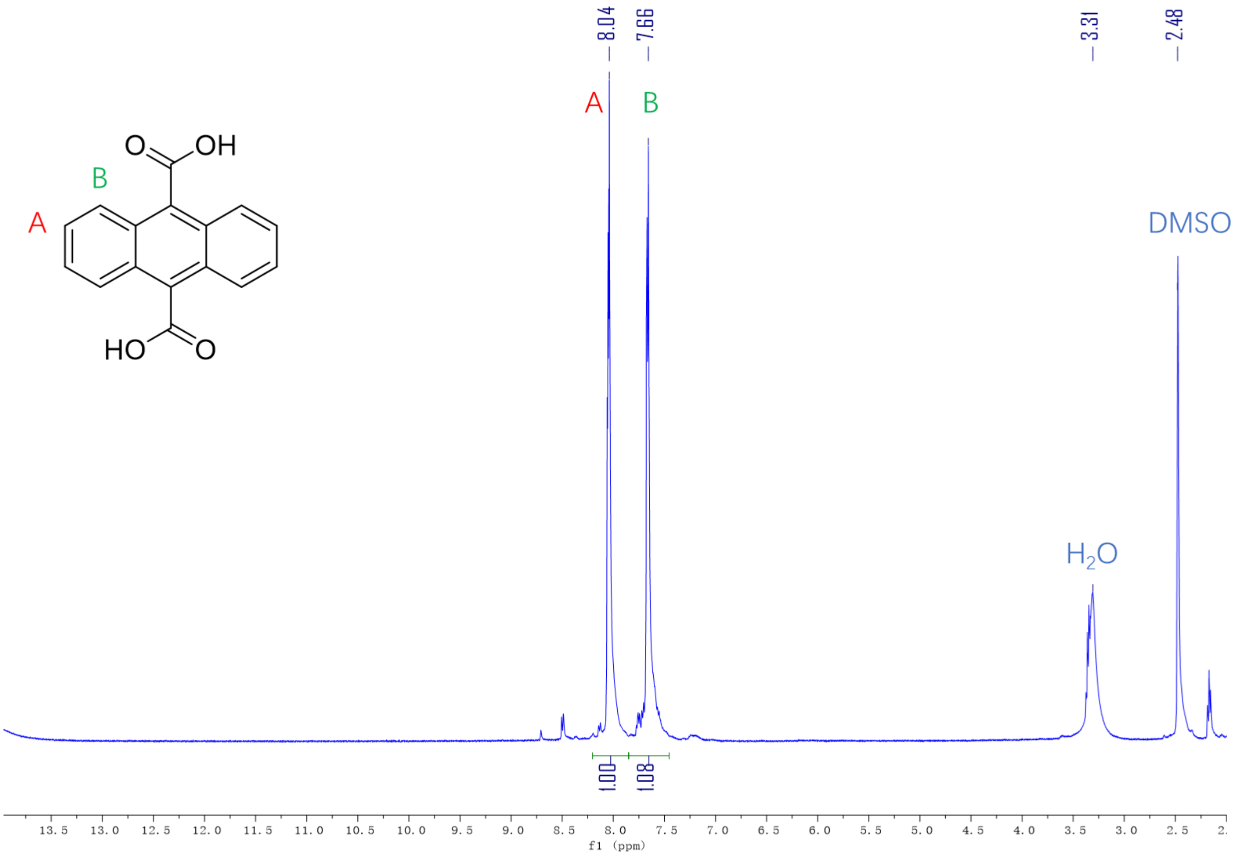

Figure S1. ^{1}H-500hz-DMSO NMR of 9,10-anthracenedicarboxylic acid (H_2adc).

S3. Single Crystal Data

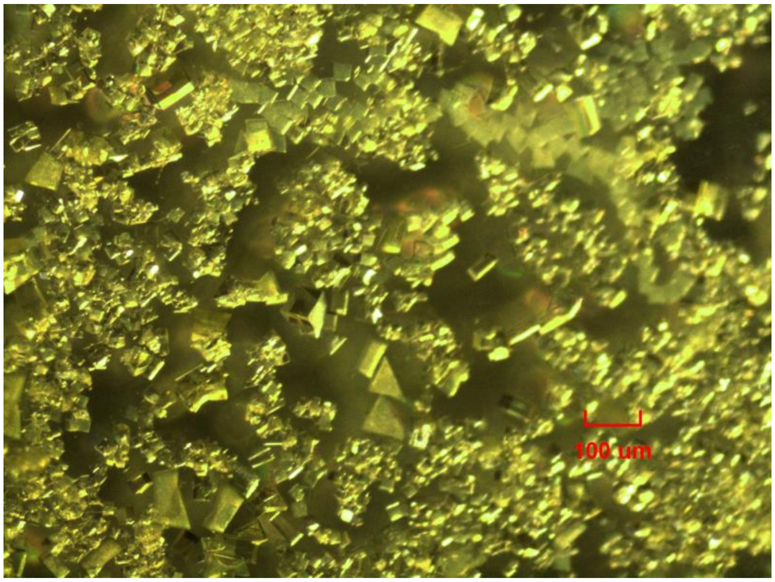

Figure S2. Optical image of cuboid shaped single crystals of $Zn_2(adc)_2(dabco)$.

Table S1. Crystal data and structure refinement parameters for $Zn_2(adc)_2(dabco)$ CCDC number: 2360909

Empirical formula	C19 H14 N O4 Zn
Formula weight	385.68
Temperature	100(2) K
Wavelength	0.7288 Å
Crystal system	Tetragonal
Space group	I4/mcm
Unit cell dimensions	a = 15.3499(10) Å α= 90°. b = 15.3499(10) Å β= 90°. c = 19.0385(19) Å γ = 90°
Volume	4485.8(7) Å^3
Z	8
Density (calculated)	1.142 Mg/m^3
Absorption coefficient	1.189 mm^{-1}
F(000)	1576
Final R indices [I>2sigma(I)]	R1 = 0.0284, wR2 = 0.0857
R indices (all data)	R1 = 0.0331, wR2 = 0.0887

S4. Powder X-Ray Diffraction (PXRD) Patterns

Powder X-ray diffraction (PXRD) analyses were performed using a Rigaku Ultima-IV-diffractometer at room temperature under Cu Kα radiation (λ = 1.5406 Å). Data were collected at room temperature in a 2θ range of 3-40°, with the operating power set to 40 kV/44 mA. The scan rate was 2°/min, with a step size of 0.2°.

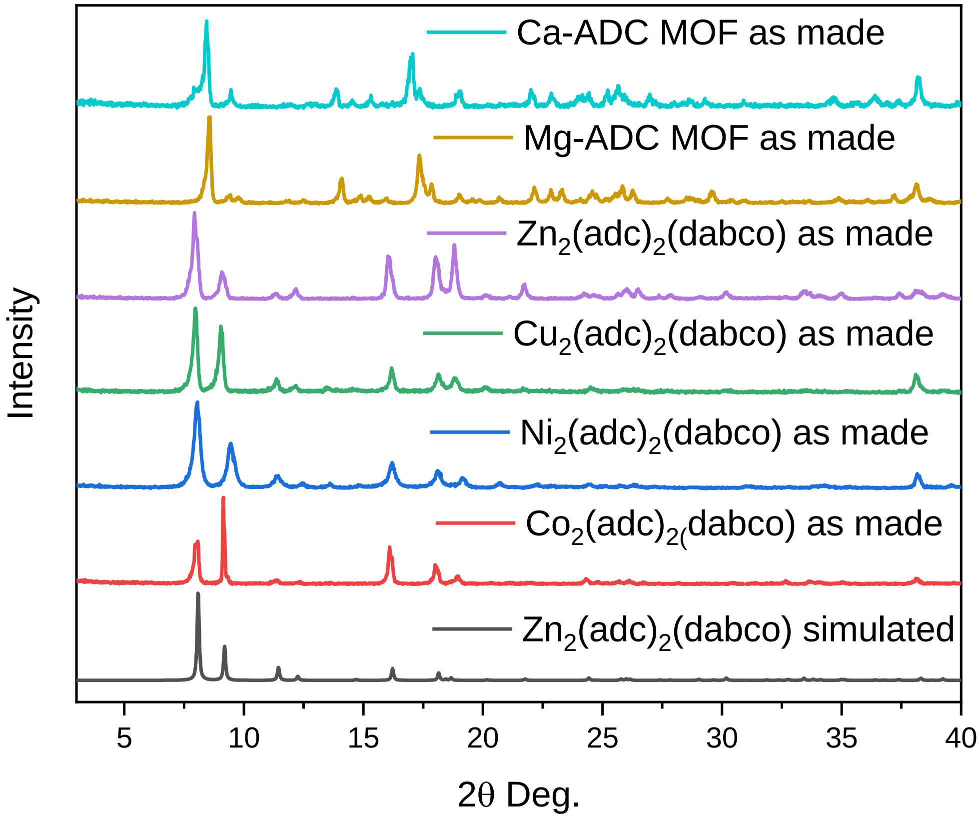

Figure S3. PXRD patterns of the as-made $M_2(adc)_2(dabco)$ (M = Zn, Cu, Ni, Co, Mg, Ca).

S5. Thermogravimetric Analysis (TGA)

Thermogravimetric analysis (TGA) was completed via a TA Instruments Q5000 under constant N_2 flow (20 mL/min). Approximately 3 mg of MOFs samples were placed into a platinum pan, which was then heated from 30-600 °C at a rate of 10 °C/min. The weight loss from MOFs were monitored over the temperature increase.

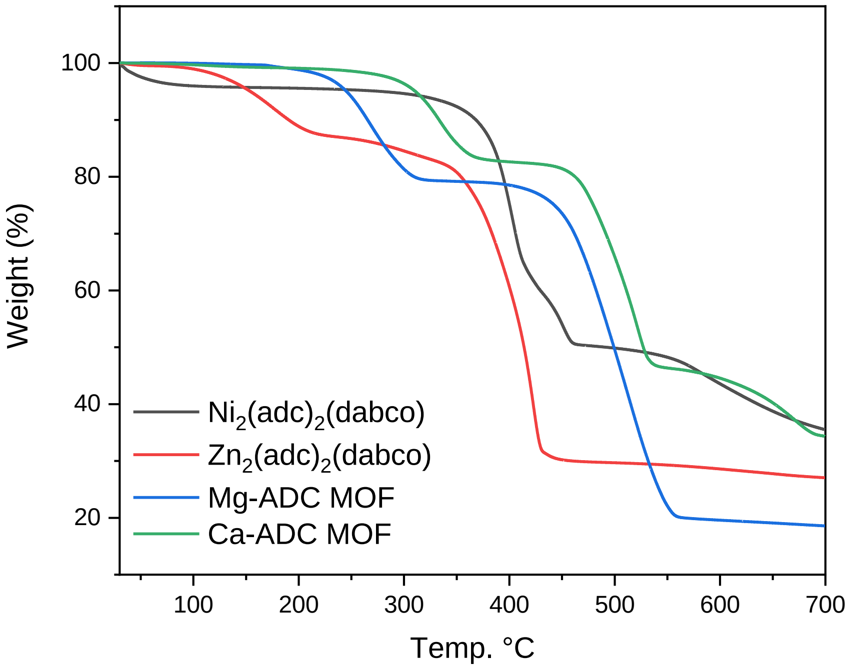

Figure S4. TG profiles of $M_2(adc)_2(dabco)$ (M = Zn, Ni, Mg, Ca).

S6. Gas Adsorption Measurements

Dynamic adsorption isotherms of CO_2 in the binary mixtures of CO_2/N_2 under humidity (RH = 50%) were collected on a gravimetric adsorption analyzer TGA Q50 (TA Instruments). The bubbler containing the water-run ultrahigh purity N_2 as the carrier gas to adjust humidity. The partial pressure of CO_2 and humidity of H_2O were adjusted by controlling the ratios of pure CO_2 and N_2 gas, and humidified N_2 gas. Gas mixtures of CO_2/N_2 (15/85) under 50% RH was generated by 15% of dry CO_2, 35% of dry N_2 and 50% of fully water saturated N_2 flow. Gas mixture of CO_2/N_2 (50/50) under 50% RH was generated by 50% of dry CO_2 50% of fully water saturated N_2 flow. Approximately 20 mg of exchanged samples was activated under a constant N_2 flow at 393 K for 60 mins. Adsorbed amounts were monitored continuously by weight changes in the sample throughout the measurements.

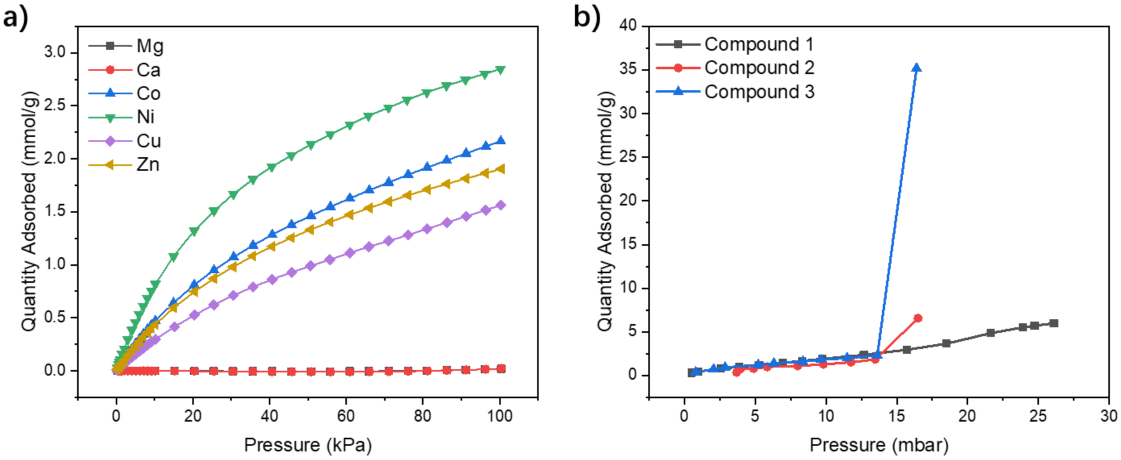

Figure S5. a) Single component CO_2 adsorption isotherms of $M_2(adc)_2(dabco)$ (M = Zn, Cu, Co, Ni, Ca, Mg) at 298 K; b) Single component water vapor adsorption isotherms for compounds **1**-**3** at 298 K.

S7. In-situ FT-IR Study

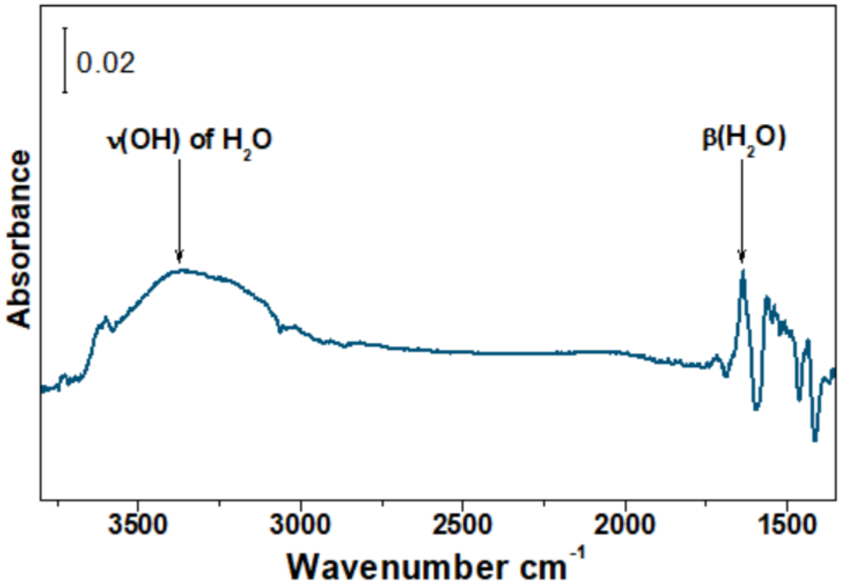

Figure S6. IR spectra of adsorbed H_2O in activated compound **1** sample. H_2O was loaded at around 11 Torr and 24 °C.

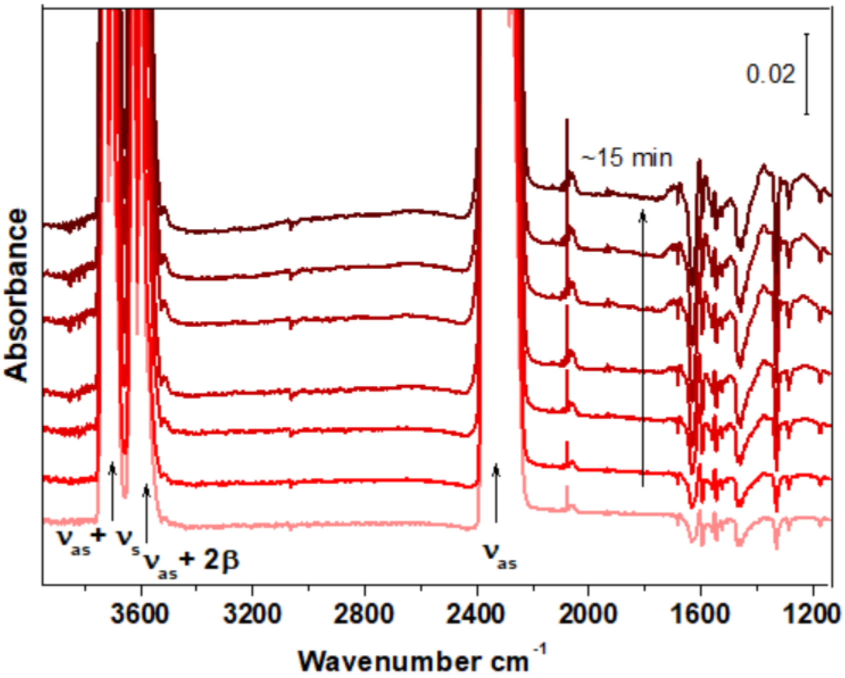

Figure S7. IR spectra of CO_2 loaded compound **1** with pre-adsorbed H_2O.

S8. Theoretical Calculation

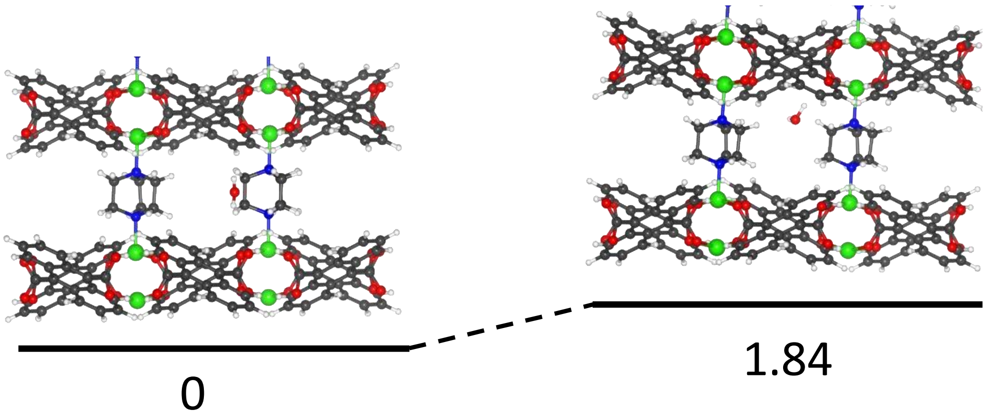

Figure S8. Two low energy binding pockets for H_2O in compound **1**. The relative energies (in kJ/mol) are given in the figure.

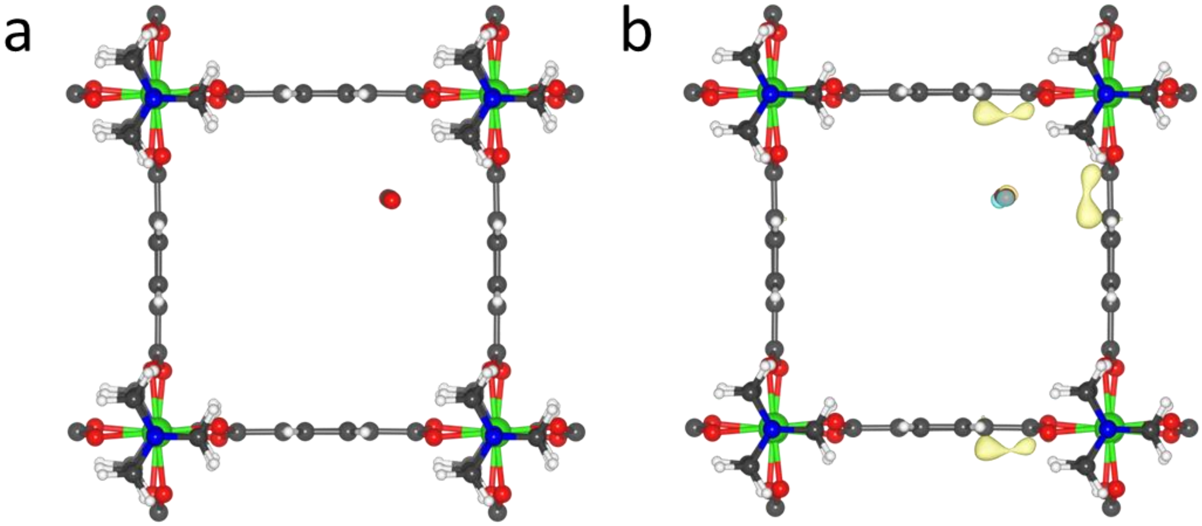

Figure S9. a) CO_2 optimum binding locations in compound **3**; b) CO_2 guest interaction with compound **3**.

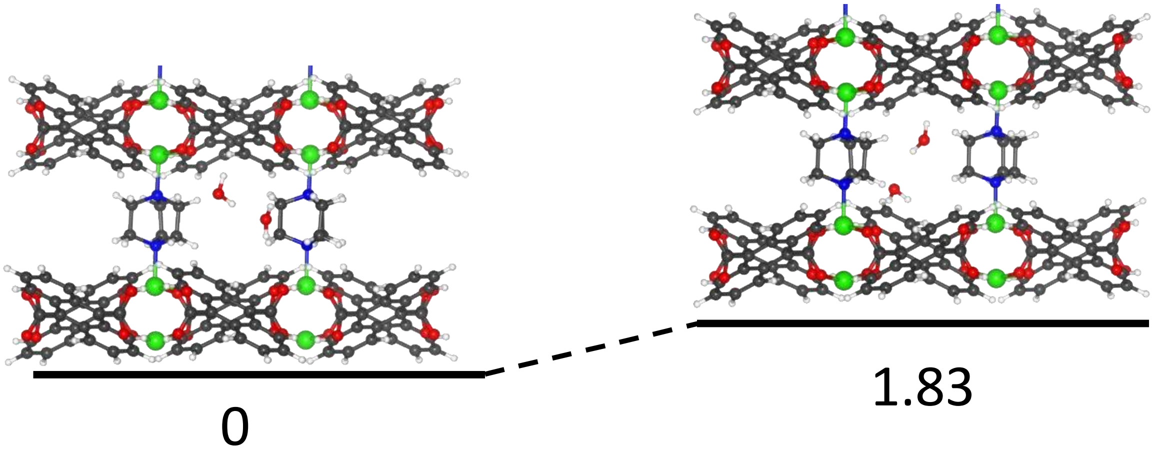

Figure S10. Low energy configurations for two H_2O molecules in compound **1**. Relative energies are given in kJ/mol.

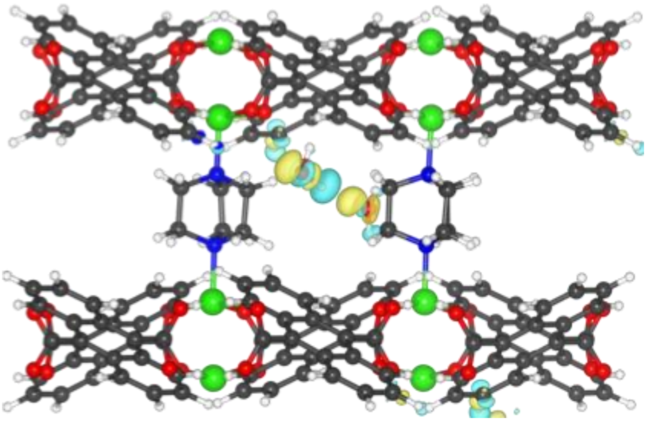

Figure S11. Water-water interactions in compound **1**. Induced charge density of one water vs compound **1** with preloaded water. The iso-value is the same as in Figure S8 [0.0005 e.Å^{-3}].

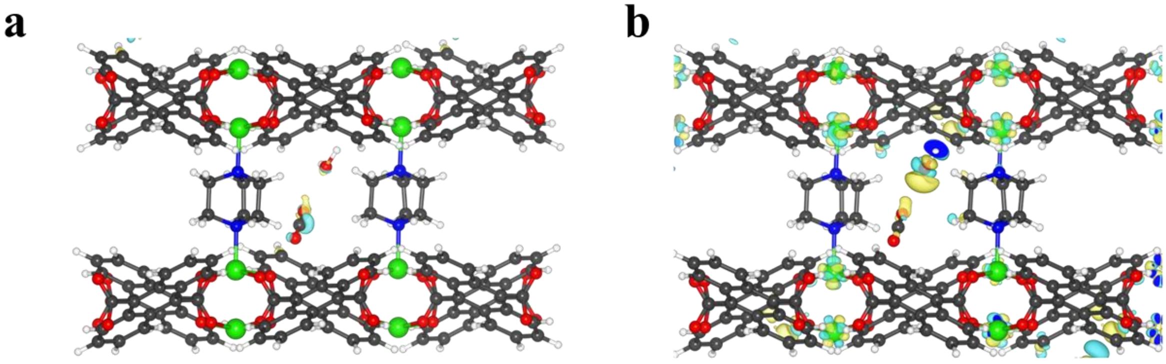

Figure S12. Induced charge density of CO_2 against preloaded H_2O (a), and charge density induced by H_2O against preloaded CO_2 (b). A noticeable synergistic effect between co-adsorbed species is visible;

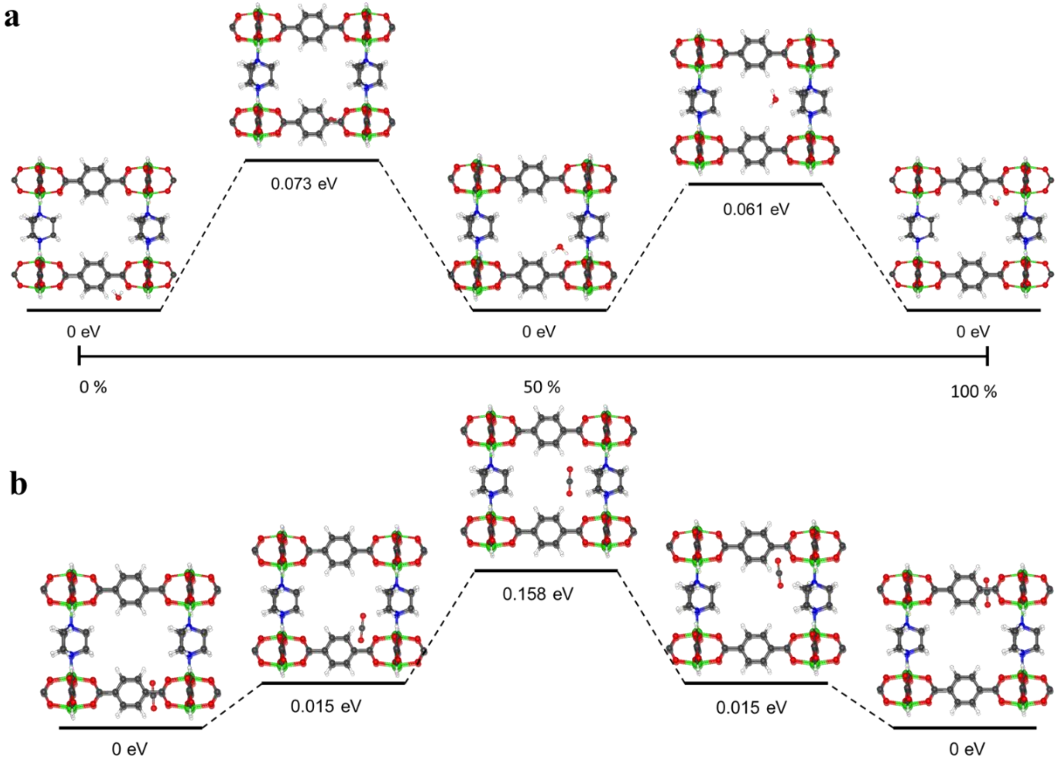

Figure S13. Example of diffusion pathway with various energy barriers for (a) H_2O and (b) CO_2 along their diffusion pathways.

S9. Adsorption Selectivity Calculations Based on IAST

Ideal adsorbed solution theory (IAST) selectivity calculation is a general method to evaluate the selectivity of binary mixtures from pure component adsorption isotherms.

$$S = \frac{X_A/X_B}{Y_A/Y_B}$$

S represents the selectivity of component A relative to B. X_A and X_B are the molar fractions of the components A and B in the adsorption phase, respectively. Y_A and Y_B are molar fractions of components A and B in the gas phase, respectively. The dual site Langmuir-Freundlich (DSLF) isotherm model was adopted to fit the adsorption isotherms of CO_2 and N_2 on the compound **1**, which is described as follow:

$$\mathrm{q} = \mathrm{q1}\frac{b1p^c}{1+b1p^c} + q2\frac{b2p^t}{1+b2p^t}$$

Where p is the equilibrium pressure of the gas phase and adsorbed phase, q1 and q2 are the saturated capacity of site a and b; b1 and b2 are the affinity coefficients of site a and b; c and t are the Freundlich exponent for the heterogeneity from an ideal homogeneous surface of site a and b, respectively.

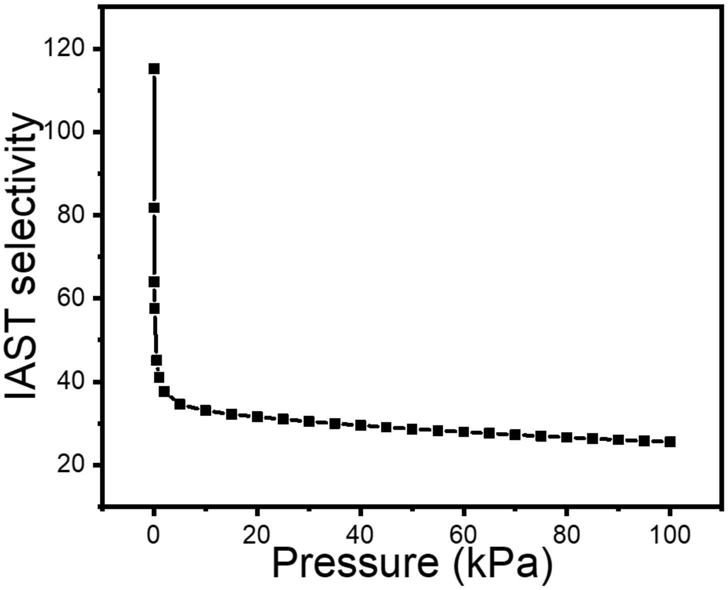

Figure S14. IAST selectivity plot for the binary CO_2/N_2 (15/85) mixture at 298K.

S10. Multiple Adsorption (Recyclability) Measurements, Long-term Stability and Error Margin Calculations

The stability and recyclability of the compound **1** have been demonstrated by six consecutive heat-swing adsorption with consistent uptake capacities. For each cycle, the uptake amounts of CO_2 at 303 K (CO_2/N_2 = 15/85) are 1.387 mmol/g, 1.380 mmol/g, 1.365 mmol/g, 1.376 mmol/g, 1.382 mmol/g, and 1.383 mmol/g, respectively. Based on this data set, we have calculated and obtained the following parameters: Mean = 1.378833, Standard Deviation = 0.007679, Uncertainty = 0.003135, Margin of error = 0.006144347.[1]

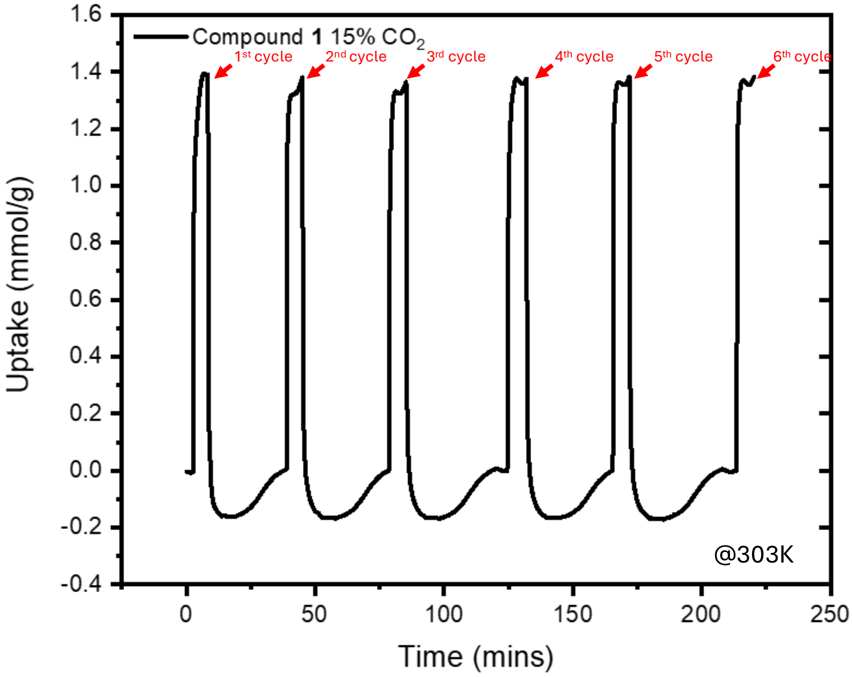

Figure S15. The CO_2 adsorption–desorption recyclability test results for compound **1**. Six consecutive adsorption cycles were carried out with a gas feeding ratio $CO_2 : N_2$ = 15 : 85 (v : v) at 303 K.

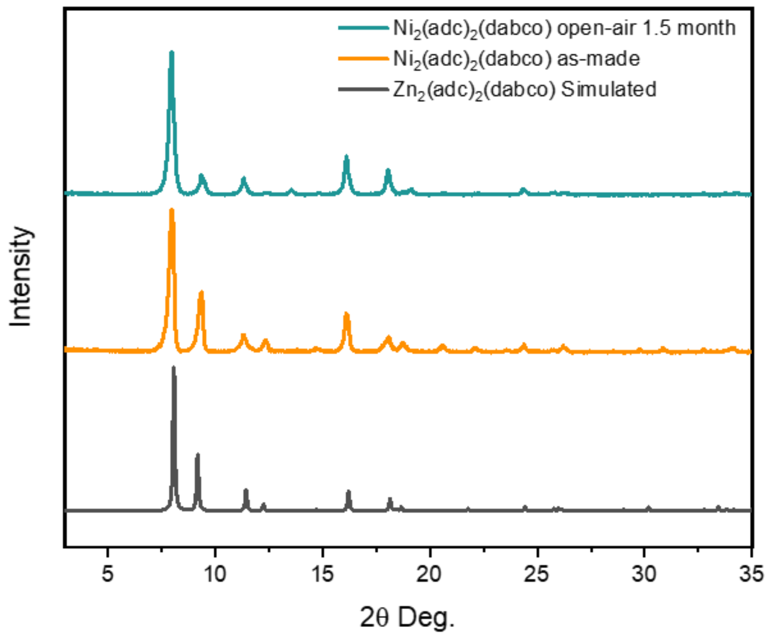

Figure S16. PXRD patten of compound **1** collected after being exposed in open-air for 1.5 month compared with those of the as-made and simulated patterns.

Table S2. Comparison of $Ni_2(adc)_2(dabco)$ with commercially viable and widely studied prototype MOF sorbents for CO_2 adsorption under dry and humid conditions

Name	CO_2 Uptake at 1 bar, 298K (Dry) (mmol/g)	CO_2 Uptake under humidity (mmol/g)	Q_{st} (kJ/mol)	Activation Temp. (°C)	Liand Cost ($/g)	Stability in water
$Ni_2(adc)_2(dabco)$	3.03	2.7 (CO_2/N_2 = 50/50, 50% RH, 303K)	25.2	100	~25	Stable
CALF-20[2, 3]	3.8	~1 (CO_2/N_2 = 20/80, 50% RH, 298K)	39	100	~4.5	Stable
ZIF-8[4]	0.85	NA	26	200	~0.5	Stable
UiO-66[5]	2.88	0.9 (CO_2/N_2 = 20/80, 40% RH, 303K)	25	150	~0.1	Stable
Mg-MOF-74[6]	8.6	1.5 (CO_2/N_2 = 15/75, 75% RH, 298K)	47	120	~37	Unstable
NbOFFIVE-Ni[7]	2.2	0.42 (pure CO_2, 74%RH, 298K)	54	150	~11	Stable
SIFSIX-3-Cu[8]	2.58	0.32 (pure CO_2, 74%RH, 298K)	54	150	~15	Stable

References:

1. M. Daszykowski, K. Kaczmarek, Y. Vander Heyden and B. Walczak, *Chemometrics and Intelligent Laboratory Systems*, 2007, **85**, 203-219.
2. J.-B. Lin, T. T. T. Nguyen, R. Vaidhyanathan, J. Burner, J. M. Taylor, H. Durekova, F. Akhtar, R. K. Mah, O. Ghaffari-Nik, S. Marx, N. Fylstra, S. S. Iremonger, K. W. Dawson, P. Sarkar, P. Hovington, A. Rajendran, T. K. Woo and G. K. H. Shimizu, *Science*, 2021, **374**, 1464-1469.
3. K. Gopalsamy, D. Fan, S. Naskar, Y. Magnin and G. Maurin, *ACS Applied Engineering Materials*, 2024, **2**, 96-103.
4. J. McEwen, J.-D. Hayman and A. Ozgur Yazaydin, *Chemical Physics*, 2013, **412**, 72-76.
5. E. Soubeyrand-Lenoir, C. Vagner, J. W. Yoon, P. Bazin, F. Ragon, Y. K. Hwang, C. Serre, J.-S. Chang and P. L. Llewellyn, *Journal of the American Chemical Society*, 2012, **134**, 10174-10181.
6. A. Kumar, C. Hua, D. G. Madden, D. O’Nolan, K.-J. Chen, L.-A. J. Keane, J. J. Perry and M. J. Zaworotko, *Chemical Communications*, 2017, **53**, 5946-5949.
7. S. Mukherjee, N. Sikdar, D. O’Nolan, D. M. Franz, V. Gascón, A. Kumar, N. Kumar, H. S. Scott, D. G. Madden, P. E. Kruger, B. Space and M. J. Zaworotko, *Sci Adv*, 2019, **5**, eaax9171.
8. O. Shekhah, Y. Belmabkhout, Z. Chen, V. Guillerm, A. Cairns, K. Adil and M. Eddaoudi, *Nature Communications*, 2014, **5**, 4228.